Layer-wise dynamic event-triggered neural network control for discrete-time nonlinear systems

Marco Sterlini, Samuele Zoboli, Sophie Tarbouriech

Layer-Wise Dynamic Event-Triggered Neural Network Control For Discrete-Time Nonlinear Systems

Marco Sterlini * **Samuele Zoboli** ** **Sophie Tarbouriech** **

* *Università di Trento, 38122 Trento, Italy, (e-mail: marco.sterlini@studenti.unitn.it)*
** *LAAS-CNRS, Université de Toulouse, CNRS, Toulouse, (e-mail: samuele.zoboli@laas.fr, sophie.tarbouriech@laas.fr)*

Abstract: Recent efforts in the control community have focused on developing methods to guarantee closed-loop stability of systems controlled by multilayer perceptron (MLP)-based policies. However, little attention has been paid to the computational capacity demand of such controllers due to frequent network evaluations. These requirements can be prohibitive in practical control applications, particularly when implemented on microcontrollers with limited computational resources. In this paper, we address this challenge by proposing a dynamic Event-Triggering Mechanism (ETM) to reduce the computational burden. Specifically, we focus on the stabilization of discrete-time Lur'e systems with input saturation. The proposed strategy reduces the evaluation frequency of the layers of the neural controller while preserving stability guarantees. The ETM is constructed using Linear Matrix Inequality (LMI)-based conditions, which leverage the known properties of activation functions and employ Finsler's lemma to reduce conservativeness. Numerical results demonstrate the effectiveness of the proposed method, achieving significant computational savings compared to state-of-the-art solutions.

Keywords: dynamic event-triggered control, neural network control, linear matrix inequalities, quadratic constraints, Lur'e systems.

1. INTRODUCTION

Recent advancements in deep learning and deep reinforcement learning highlighted the growing potential of Neural Networks (NNs) as effective solutions in automatic control, emerging as viable alternatives to traditional controllers. As a consequence, substantial efforts have been directed towards the derivation of training methods ensuring stability of the closed loop under the NN controller, e.g. (Chow et al., 2018; Sun et al., 2021; Yang et al., 2024; Zoboli et al., 2021). Particularly interesting are methods inspired by robust control theory, that use Integral Quadratic Constraints to model uncertainties and activation functions and employ semidefinite programming and LMI-based conditions to enforce and certify stability (Junnarkar et al., 2024a; Wang and Manchester, 2022; Yin et al., 2021). Most of these studies focus on guaranteeing closed-loop stability throughout the training process, which is typically performed offline and is less constrained by computational resource limitations. However, in addition to stability guarantees, computational efficiency is crucial in real-world applications. In practical applications, control laws are executed on microcontrollers with limited computational capacity, and the highly nested nonlinear structure of NNs can become increasingly prohibitive as the network depth grows. Yet, much less attention has been paid to such a problem.

† Research partly supported by ANR via grant OLYMPIA, number ANR-23-CE48-0006.

Event-triggered control (ETC) has proven to be an effective paradigm to address this issue by updating control actions only when necessary (Girard, 2015; Tabuada, 2007). This reduces computational overhead, making ETC highly suitable for resource-constrained environments. For example, ETC can be used to define lower-priority control tasks in multitask scenarios, where event-based signals serve as *interrupts*, saving computational resources by avoiding unnecessary nonlinear function evaluations and freeing up processing time for other tasks (Dimarogonas and Johansson, 2009). Within the context of NNs, ETC has traditionally focused on state transmission during learning or controller sampling, e.g., (Hu et al., 2016; Mu et al., 2022). Approaches combining ETC and NN-based control to reduce layers evaluations appeared in (de Souza et al., 2023a,b), where ETMs are integrated into trained neural networks to selectively determine which portions of it must be evaluated to ensure stability. However, the proposed methods become increasingly conservative as the complexity of the closed-loop system grows, particularly with the addition of more layers in the controllers.

In this paper, we build on these works and propose a layer-wise dynamic ETM strategy that improves existing approaches in three main directions. First, we show how input saturated systems can be tackled by these family of methods via a simple controller reformulation. Second, we significantly reduce the conservatism of the proposed solution by leveraging Finsler's lemma to derive unstructured proxies for local sector conditions (Boyd et al., 1994;

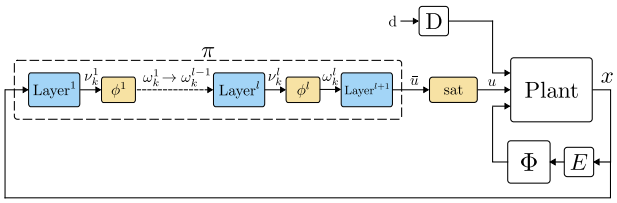

Fig. 1. Feedback system

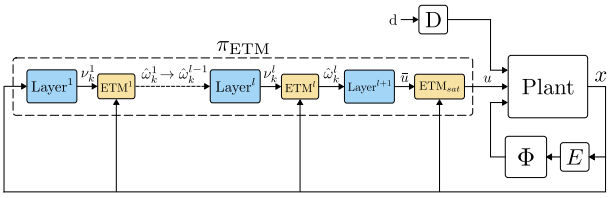

Fig. 2. Feedback system subject to ETM in the controller

Meijer et al., 2024; Tarbouriech et al., 2011). Third, we introduce a dynamic triggering threshold to further reduce the total number of layers evaluations (Girard, 2015). We also discuss possible optimization procedure to improve performance of the overall scheme and numerically validate the proposed methodology by comparing it with the results in (de Souza et al., 2023a) and (Tarbouriech et al., 2024). Our approach significantly reduces update rates and expands the region-of-attraction (ROA) approximation.

Notation: $\mathbb{N}, \mathbb{R}^n, \mathbb{R}^{n\times m}$ denote the set of natural non-negative integers, the set of real vectors of dimension n and the set of real matrices of dimension $n \times m$, respectively. I_n denotes the identity matrix of dimension $n \times n$. For any matrix A, $A^\top$ is its transpose. For any square matrix A, we define the operator $\mathrm{He}\{A\} = A + A^\top$. $\mathtt{diag}(A_1, A_2)$ is a block-diagonal matrix with blocks A_1 and A_2. $\mathrm{col}\left(a^1, \ldots, a^n\right)$ is the column vector of the elements a^i for all $i = 1, \ldots, n$. For a partitioned matrix, the symbol $\star$ stands for symmetric blocks. $\mathbf{1}_n = \mathrm{col}\,(1, \ldots, 1) \in \mathbb{N}^{n\times 1}$. We identify with subscript i the i^{th} element of a vector or the i^{th} row of a matrix. We identify with superscript i the objects related to the i^{th} layer of the neural network.

2. PROBLEM FORMULATION

We consider a discrete-time nonlinear system of the form

$$x^+ = Ax + B\mathtt{sat}(\bar{u}) + C\Phi(Ex) + Dd \tag{1}$$

where $x \in \mathbb{R}^{n_x}$ is the state vector, $\bar{u} \in \mathbb{R}^{n_u}$ is the input vector, $d \in \mathbb{R}^{n_d}$ is a constant reference (or disturbance) signal, $\Phi : \mathbb{R}^{n_q} \to \mathbb{R}^{n_q}$ is a decentralized, memory-less nonlinearity and $\mathtt{sat} : \mathbb{R}^{n_u} \to \mathbb{R}^{n_u}$ is the symmetric component-wise saturation function

$$\mathtt{sat}_i(\bar{u}) = \mathtt{sign}(\bar{u}_i)\min(|\bar{u}_i|, \mathtt{u}_i), \quad i = 1, \ldots, n_u,$$

with $\mathtt{u}_i$ the saturation limits for the i^{th} element of the input vector. The input $\bar{u}$ is generated by a stabilizing MLP-controller π, see Figure 1, which makes the point x_* Locally Exponentially Stable (LES). We assume the nonlinearity Φ satisfies a local quadratic abstraction with respect to x_*. Specifically, we assume the following.

Assumption 1. There exist element-wise positive vectors $\underline{\mu}, \bar{\mu} > 0 \in \mathbb{R}^{n_q}$ and matrices $S, Q, W \in \mathbb{R}^{n_q\times n_q}$ such that

$$\begin{bmatrix} y - y_* \\ \Phi(y) - \Phi(y_*) \end{bmatrix}^\top \begin{bmatrix} S & Q \\ \star & W \end{bmatrix} \begin{bmatrix} y - y_* \\ \Phi(y) - \Phi(y_*)) \end{bmatrix} \geq 0 \tag{2}$$

for all $y = Ex$ such that $y \in \bar{\mathcal{S}}$ with

$$\bar{\mathcal{S}} = \left\{ y \in \mathbb{R}^{n_q} : -\underline{\mu}_i \leq y_i - y_i* \leq \bar{\mu}_i, i = 1, \ldots, n_q \right\}. \tag{3}$$

The controller π is implemented as an MLP with l layers, each containing n_{ϕ^i} neurons for $i = 1, \ldots, l$. More specifically, the input $\bar{u}$ is computed as

$$\begin{aligned} \omega^0(k) &= x(k), \\ \nu^i(k) &= W^i\omega^{i-1}(k) + b^i, \quad i = 1, \ldots, l, \\ \omega^i(k) &= \phi^i(\nu^i(k)), \\ \bar{u}(k) &= W^{l+1}\omega^l(k) + b^{l+1}, \end{aligned} \tag{4}$$

where $\nu^i(k) \in \mathbb{R}^{n_{\phi^i}}$ represents the input to the i^{th} activation function $\phi^i : \mathbb{R}^{n_{\phi^i}} \to \mathbb{R}^{n_{\phi^i}}$, and $\omega^i(k) \in \mathbb{R}^{n_{\phi^i}}$ denote the forwarded quantities. The weights $W^i \in \mathbb{R}^{n_{\phi^i}\times n_{\phi^{i-1}}}$ and biases $b^i \in \mathbb{R}^{n_{\phi^i}}$ define the affine transformation of each layer. The application of the activation function is element-wise and is denoted as $\phi^i(\nu^i(k)) = \mathrm{col}(\varphi(\nu^i_1(k)), \ldots, \varphi(\nu^i_{n_{\phi^i}}(k)))$, where $\varphi : \mathbb{R} \to \mathbb{R}$ is a scalar activation function that is assumed to be symmetric and identical for every neuron. Similarly to (de Souza et al., 2023a; Yin et al., 2021), the controller policy can be expressed in a condensed form by introducing the augmented vectors

$$\bar{\nu} = \begin{bmatrix} \nu^1 \\ \vdots \\ \nu^l \end{bmatrix}, \ \bar{\omega} = \begin{bmatrix} \omega^1 \\ \vdots \\ \omega^l \end{bmatrix}, \ \bar{\phi} = \begin{bmatrix} \phi^1(\nu^1) \\ \vdots \\ \phi^l(\nu^l) \end{bmatrix}. \tag{5}$$

By defining $n_{\bar{\phi}} = \sum_{i=1}^{l} n_{\bar{\phi}^i}$ and $\bar{\phi} : \mathbb{R}^{n_{\bar{\phi}}} \to \mathbb{R}^{n_{\bar{\phi}}}$ representing the combined nonlinearity, we have $\bar{\omega} = \bar{\phi}(\bar{\nu})$. Finally, the equations in (4) can be reformulated as

$$\begin{bmatrix} \bar{u}(k) \\ \bar{\nu}(k) \end{bmatrix} = \overline{N} \begin{bmatrix} x(k) \\ \bar{\omega}(k) \\ 1 \end{bmatrix},$$

where

$$\overline{N} = \left[\begin{array}{c|cccc|c} 0 & 0 & \ldots & 0 & W^{l+1} & b^{l+1} \\ \hline W^1 & 0 & \ldots & 0 & 0 & b^1 \\ 0 & W^2 & \ldots & 0 & 0 & b^2 \\ \vdots & \vdots & \ddots & \vdots & \vdots & \vdots \\ 0 & 0 & \ldots & W^l & 0 & b^l \end{array}\right]. \tag{6}$$

The above formulation can be extended to include the input saturation function as a virtual additional layer of the controller π via the change of input $u = \mathtt{sat}(\bar{u}) = \phi^{l+1}(\nu^{l+1}) = \omega^{l+1}$. Therefore, the system dynamics are rewritten as

$$x^+ = Ax + Bu + C\Phi(Ex) + Dd, \tag{7}$$

where

$$\begin{bmatrix} u(k) \\ \nu(k) \end{bmatrix} = N \begin{bmatrix} x(k) \\ \omega(k) \\ 1 \end{bmatrix}, \nu = \begin{bmatrix} \bar{\nu} \\ \bar{u} \end{bmatrix}, \omega = \begin{bmatrix} \bar{\omega} \\ \omega^{l+1} \end{bmatrix}, \phi = \begin{bmatrix} \bar{\phi} \\ \mathtt{sat}(\bar{u}) \end{bmatrix}.$$

with $n_\phi = n_{\bar{\phi}} + n_u = n_{\bar{\phi}} + n_{\phi^{l+1}}$ and

$$N = \left[\begin{array}{c|c|ccc|c} 0 & 0 & \dots & 0 & \mathrm{I}_{n_u} & 0 \\ \hline W^1 & 0 & \dots & 0 & 0 & b^1 \\ 0 & W^2 & \dots & 0 & 0 & b^2 \\ \vdots & \vdots & \ddots & \vdots & \vdots & \vdots \\ 0 & 0 & \dots & W^{l+1} & 0 & b^{l+1} \end{array}\right] = \left[\begin{array}{c|c|c} N_{ux} & N_{u\omega} & N_{ub} \\ \hline N_{\nu x} & N_{\nu\omega} & N_{\nu b} \end{array}\right]. \tag{8}$$

Given system (7), our objective is to design an ETM strategy exploiting properties of the activation functions to decide if a layer's output has to be computed. However, this requires knowledge of the equilibrium point $(x_*, u_*, \nu_*, \omega_*)$. By following steps similar to (Tarbouriech et al., 2024, Lemma 2), the values of u_*, ν_*, ω_* can be analytically derived for any given x_*. More specifically, let us introduce the following matrices

$$\begin{aligned} R &= (\mathrm{I}_{n_\phi} - N_{\nu\omega})^{-1}, \\ R_\omega &= N_{ux} + N_{u\omega} R N_{\nu x}, \\ R_b &= N_{u\omega} R N_{\nu b} + N_{ub}. \end{aligned} \tag{9}$$

Given the lower triangular structure of $N_{\nu\omega}$, the matrix $\mathrm{I}_{n_\phi} - N_{\nu\omega}$ is always invertible and R is well-defined. Then, u_*, ν_*, ω_* are defined as functions of x_* by the following relations

$$\begin{aligned} \omega_* &= \nu_*, \\ \nu_* &= R N_{\nu x} x_* + R N_{\nu b}, \\ u_* &= R_\omega x_* + R_b. \end{aligned} \tag{10}$$

However, differently from (Tarbouriech et al., 2024), given a constant disturbance d_* the equilibrium system's state is the solution of an implicit equation due to the presence of Φ. Therefore, we now propose a numerical procedure to compute x_*. Specifically, an approximation can be found by solving the following minimization problem

$$x_* = \min_x \left[(A + B R_\omega - \mathrm{I}_{n_x}) x + C\Phi(Ex) + D d_* + B R_b \right]. \tag{11}$$

To design the triggering function, we aim to exploit known properties of the activation functions. In what follows, we assume all activation functions have been selected as saturations (with possibly different limits). This choice allows treating the controller and input saturation nonlinearities at once in the stability analysis, while exploiting known and general local sector conditions. We remark that symmetric saturations can be interpreted as piecewise linear approximations of the common tanh activation functions. However, they satisfy well-established local sector conditions(Tarbouriech et al., 2011). We now recall (Tarbouriech et al., 2024, Lemma 3) which provides local sector conditions for NN layers with saturations as activation functions.

Lemma 1. *For $i \in \{1, \dots, l+1\}$, let $\bar{\mathrm{v}}^i$ be the vector of saturation levels of the i^{th} layer and consider a matrix $G^i \in \mathbb{R}^{n_{\phi^i} \times n_x}$. If x belongs to the set*

$$S^i = \left\{ x \in \mathbb{R}^{n_x} : -\bar{\mathrm{v}}^i - \nu_*^i \le G^i (x - x_*) \le \bar{\mathrm{v}}^i - \nu_*^i \right\}, \tag{12}$$

then the following quadratic constraint holds for any diagonal positive definite matrix $T^i \in \mathbb{R}^{n_{\phi^i} \times n_{\phi^i}}$

$$\left[\nu^i - \omega^i\right]^\top T^i \left[G^i (x - x_*) - (\omega^i - \omega_*^i) \right] \le 0. \tag{13}$$

In the scenario of (7), we have $\bar{\mathrm{v}}^{l+1} = \mathtt{u}$. Moreover, the set where all local sector conditions are satisfied is denoted as $\mathcal{S} = \cap_{i=1}^{l+1} \mathcal{S}^i$.

3. MAIN RESULTS

To reduce the computational burden imposed by the evaluation of nonlinear activation functions at each timestep, we propose an ETM strategy (Postoyan et al., 2015; Tabuada, 2007). As shown by (7), the input-saturated closed-loop dynamics can be interpreted as non-saturated ones under an $(l+1)$-layers MLP controller. Therefore, inspired by (Tarbouriech et al., 2024), we assign a triggering mechanism to each MLP layer and the input saturation function, see Figure 2. Similarly to (Tarbouriech et al., 2024), we design the triggering law by exploiting local sector conditions satisfied by such nonlinearities. However, we introduce three main improvements. First, we circumvent constraints imposed by the highly structured form of (13) through Finsler's lemma, e.g., (Boyd et al., 1994; Meijer et al., 2024; Tarbouriech et al., 2011). This greatly improves the flexibility of the ETM design conditions and enhances the mechanism's performance. Second, we introduce a dynamic triggering threshold (Girard, 2015). This further increases inter-event time and reduces the total amount of events. Third, we treat input-saturated systems by including such input constraints as an additional layer of the MLP.

Before presenting the ETM scheme, we introduce some useful notation. We denote by $\widehat{\omega}^i$ the last forwarded output of the i^{th} layer and ω^i the current output after applying the activation function. Note that due to the triggering mechanism, $\widehat{\omega}^i = \omega^i$ only at events. Given (4), the triggered controller now reads

$$\begin{aligned} \widehat{\omega}^0(k) &= x(k), \\ \nu^i(k) &= W^i \widehat{\omega}^{i-1}(k) + b^i, \qquad i = 1, \dots, l, \\ \widehat{\omega}^i(k) &= \phi^i(\nu^i(k)), \\ u(k) &= \mathtt{sat}(\bar{u}(k)) = \mathtt{sat}(W^{l+1} \widehat{\omega}^l(k) + b^{l+1}). \end{aligned} \tag{14}$$

When studying saturation functions, it is useful to refer to their dead-zone reformulation (Tarbouriech et al., 2011). The dead-zone vectors are defined as $\psi^i = \nu^i - \omega^i$ and $\widehat{\psi}^i = \nu^i - \widehat{\omega}^i$. We also denote incremental variables relative to their equilibrium with a tilde notation, e.g., $\tilde{x} = x - x_*, \tilde{\Phi} = \Phi(Ex) - \Phi(Ex_*)$. Given (10) and since $\psi_* = \nu_* - \omega_* = 0$, we have $\tilde{\psi} = \psi$. Therefore, we have

$$\begin{aligned} \tilde{u} &= R_\omega \tilde{x} - N_{u\omega} R \tilde{\psi} \\ \tilde{\nu} &= R N_{\nu x} \tilde{x} + (\mathrm{I}_{n_\phi} - R) \tilde{\psi}. \end{aligned} \tag{15}$$

We define $\xi^i = \mathrm{col}(\tilde{x}, \tilde{\psi}^i, \tilde{\nu}^i)$ and $\widehat{\xi}^i = \mathrm{col}(\tilde{x}, \widetilde{\widehat{\psi}^i}, \tilde{\nu}^i) \in \mathbb{R}^{n_{\xi^i}}$ with $n_{\xi^i} = n_x + 2n_{\phi^i}$. We also write the extended vectors $\xi = \mathrm{col}(\tilde{x}, \tilde{\psi}, \tilde{\nu})$, $\widehat{\xi} = \mathrm{col}(\tilde{x}, \widetilde{\widehat{\psi}}, \tilde{\nu}) \in \mathbb{R}^{n_\xi}$, where $n_\xi = n_x + 2n_\phi$. Finally, we define $Z^i = T^i G^i \in \mathbb{R}^{n_{\phi^i} \times n_x}$ for each $i = 1, \dots, l+1$. Then, the local sector condition in (13) can be rewritten without loss of generality as

$$\begin{aligned} (\tilde{\psi}^i)^\top T^i \left[G^i \tilde{x} + \tilde{\psi}^i - \tilde{\nu}^i \right] &= {\xi^i}^\top \begin{bmatrix} 0 & 0 & 0 \\ Z^i & T^i & -T^i \\ 0 & 0 & 0 \end{bmatrix} \xi^i = \\ &= {\xi^i}^\top \Omega^i \xi^i \le 0, \end{aligned} \tag{16}$$

for all $\xi \in \mathcal{S}_\xi$ with

$$\mathcal{S}_\xi = \{ \xi \in \mathbb{R}^{n_\xi} : \xi = \mathrm{col}(\tilde{x}, \tilde{\psi}, \tilde{\nu}), x \in \mathcal{S} \}.$$

We now introduce the proposed ETM strategy.

3.1 Dynamic event-triggering mechanism

The proposed ETM operates by triggering an event to update the current layer and propagate its value throughout the network. By introducing the triggered variables $\widehat{\omega}^i$ as in (14) for $i = 1, \dots, l+1$, the dynamic ETM strategy is defined as

$$\widehat{\omega}^i(k) = \begin{cases} \phi^i(\nu^i(k)) & \text{if } \Psi^i(\widehat{\xi}(k)) > \rho^i(\eta(k)), \\ \widehat{\omega}^i(k-1) & \text{otherwise,} \end{cases} \tag{17}$$

where $\Psi^i : \mathbb{R}^{n_\xi} \to \mathbb{R}$ is the triggering function for layer i and $\rho^i : \mathbb{R}^{l+1} \to \mathbb{R}_{\geq 0}$ is the dynamic threshold function driven by the dynamic ETM state $\eta \in \mathbb{R}^{l+1}_{\geq 0}$. Note that with the triggering strategy (17) events are independent and can be asynchronous. As such, some portions of the network can be updated without propagating their renewed output to the end of the network, whose output value will be recomputed only once a corresponding event is generated. In other words, each layer's ETM may store values corresponding to different timesteps with respect to other layers' ETM.

In what follows, we consider a linear, decentralized dynamic threshold function $\rho^i(\eta) = \rho^i \eta^i$ with $\rho^i > 0$ for all $i = 1, \dots, l+1$. By defining the aggregate vectors $\boldsymbol{\eta} = \mathrm{col}(\eta^1, \dots, \eta^{l+1})$, $\boldsymbol{\Psi} = \mathrm{col}(\Psi^1(\widehat{\xi}), \dots, \Psi^{l+1}(\widehat{\xi}))$ and the matrix $\mathbf{R} = \mathrm{diag}(\rho^1, \dots, \rho^{l+1})$, the component-wise aggregate triggering condition reads

$$\boldsymbol{\Psi} > \mathbf{R}\boldsymbol{\eta}.$$

We select the ETM state dynamics

$$\boldsymbol{\eta}^+ = \mathbf{R}\boldsymbol{\eta} - \boldsymbol{\Psi}. \tag{18}$$

The design of the triggering function is inspired by (Tarbouriech et al., 2024). There, the authors exploit local sector conditions to discriminate whether an event should be triggered. In other words, adapting their static ETM scenario, $\Psi^i(\widehat{\xi^i}) = (\widehat{\xi^i})^\top \Omega^i \widehat{\xi^i}$ with Ω^i as in (16) and $\rho^i = 0$ for all $i = 1, \dots, l+1$. By letting $\Pi^i \in \mathbb{R}^{n_{\xi^i} \times n_\xi}$ be a projection matrix such that $\xi^i = \Pi^i \xi$ for $i = 1, \dots, l+1$, the resulting component-wise aggregate triggering condition is $\boldsymbol{\Psi}_{\boldsymbol{\Omega}} > 0$, where

$$\begin{aligned} \boldsymbol{\Psi}_{\boldsymbol{\Omega}} &= \left(\mathrm{I}_{l+1} \otimes \widehat{\xi}\right)^\top \boldsymbol{\Omega} \left(\mathbf{1}_{l+1} \otimes \widehat{\xi}\right), \\ \boldsymbol{\Omega} &= \mathrm{diag}({\Pi^1}^\top \Omega^1 \Pi^1, \dots, {\Pi^{l+1}}^\top \Omega^{l+1} \Pi^{l+1}). \end{aligned} \tag{19}$$

While interesting, such a choice is limited by the highly structured form of Ω^i, resulting in more conservative designs the more layers are added to the network. Therefore, we propose a triggering function similarly related to the activation functions nonlinearity properties, yet free from any structural constraint. We now present a technical lemma allowing the definition of an unstructured triggering function by means of Finsler's lemma.

Lemma 2. *If there exist matrices $X^i \in \mathbb{R}^{n_{\xi^i} \times n_{\xi^i}}$, $N_1^i \in \mathbb{R}^{n_x \times n_\phi}, N_2^i, N_3^i \in \mathbb{R}^{n_\phi \times n_\phi}, Z^i \in \mathbb{R}^{n_{\phi^i} \times n_x}$ and diagonal matrices $T^i \succ 0 \in \mathbb{R}^{n_{\phi^i} \times n_{\phi^i}}$ such that*

$$\begin{aligned} &{\Pi^i}^\top \mathrm{He}\left\{X^i - \Omega^i\right\} \Pi^i \\ &\quad + \mathrm{He}\left\{ \begin{bmatrix} N_1^i \\ N_2^i \\ N_3^i \end{bmatrix} \begin{bmatrix} RN_{\nu x} & \mathrm{I}_{n_\phi} - R & -\mathrm{I}_{n_\phi} \end{bmatrix} \right\} \preceq 0, \end{aligned} \tag{20}$$

for each $i = 1, \dots, l+1$ with Ω^i as in (16), then

$$ {\xi^i}^\top X^i \xi^i \leq {\xi^i}^\top \Omega^i \xi^i \quad \forall \xi^i \in \mathbb{R}^{n_{\xi^i}}, \, \forall i = 1, \dots, l+1. \tag{21}$$

Proof: Note that, by the second equality in (15),

$$\begin{bmatrix} RN_{\nu x} & \mathrm{I}_{n_\phi} - R & -\mathrm{I}_{n_\phi} \end{bmatrix} \xi = 0$$

Therefore, if (20) holds for all $i = 1, \dots, l+1$, pre- and post-multiplying it by ξ and its transpose, we obtain

$$\xi^\top {\Pi^i}^\top \mathrm{He}\left\{X^i - \Omega^i\right\} \Pi^i \xi \leq 0, \quad i = 1, \dots, l+1.$$

Since $\xi^i = \Pi^i \xi$, we have

$$\begin{aligned} {\xi^i}^\top (X^i + {X^i}^\top) \xi^i &\leq {\xi^i}^\top (\Omega^i + {\Omega^i}^\top) \xi^i \\ 2{\xi^i}^\top X^i \xi^i &\leq 2{\xi^i}^\top \Omega^i \xi^i \\ {\xi^i}^\top X^i \xi^i &\leq {\xi^i}^\top \Omega^i \xi^i, \quad i = 1, \dots, l+1. \end{aligned}$$

thus concluding the proof. □

Lemma 2 has two interesting consequences. First, we can select the unstructured matrices X^i as a proxy for the sector conditions defined by Ω^i. Indeed, if ${\xi^i}^\top \Omega^i \xi^i \leq 0$ for all $\xi \in \mathcal{S}_\xi$, then (21) ensures ${\xi^i}^\top X^i \xi^i \leq 0$ inside the same set. Second, in view of (17), inequality (21) highlights the triggering function $\Psi^i_X(\widehat{\xi}) = (\widehat{\xi^i})^\top X^i \widehat{\xi^i}$ is less prone to event generation with respect to $\Psi^i_\Omega(\widehat{\xi}) = (\widehat{\xi^i})^\top \Omega^i \widehat{\xi^i}$. Motivated by these advantages, we propose the ETM component-wise aggregate triggering condition

$$\begin{aligned} \boldsymbol{\Psi}_{\mathbf{X}} &> \mathbf{R}\boldsymbol{\eta}, \\ \boldsymbol{\Psi}_{\mathbf{X}} &= \left(\mathrm{I}_{l+1} \otimes \widehat{\xi}\right)^\top \mathbf{X} \left(\mathbf{1}_{l+1} \otimes \widehat{\xi}\right), \\ \mathbf{X} &= \mathrm{diag}({\Pi^1}^\top X^1 \Pi^1, \dots, {\Pi^{l+1}}^\top X^{l+1} \Pi^{l+1}), \end{aligned} \tag{22}$$

with X^i derived from Lemma 2, thus obtaining the ETM state dynamics

$$\boldsymbol{\eta}^+ = \mathbf{R}\boldsymbol{\eta} - \boldsymbol{\Psi}_{\mathbf{X}}. \tag{23}$$

Remark 1. *For all non-negative initial conditions $\boldsymbol{\eta}(0)$, the ETM variable $\boldsymbol{\eta}$ can be proven to remain non-negative. Indeed, if an event is not generated, for a non-negative initial condition $\boldsymbol{\eta}$ inequality (22) implies*

$$\boldsymbol{\eta}^+ = \mathbf{R}\boldsymbol{\eta} - \boldsymbol{\Psi}_{\mathbf{X}} \geq 0.$$

Similarly, at events we have $\widehat{\xi} = \xi$ and therefore (21) yields

$$\boldsymbol{\eta}^+ = \mathbf{R}\boldsymbol{\eta} - \boldsymbol{\Psi}_{\mathbf{X}} \geq \mathbf{R}\boldsymbol{\eta} - \underbrace{\boldsymbol{\Psi}_{\boldsymbol{\Omega}}}_{\leq 0} \geq 0.$$

By induction, if $\boldsymbol{\eta}(0) \geq 0$, then $\boldsymbol{\eta}(k) \geq 0$ for all $k \geq 0$.

3.2 Stability analysis

In this section, we analyze closed-loop stability of the proposed ETM scheme and provide LMI-based conditions for the ETM matrices co-design. The solution to the proposed LMIs provides the matrices $\mathbf{X}$ and $\mathbf{R}$ guaranteeing local stability of the desired equilibrium, along with an estimate of its Region of Attraction (ROA).

To this aim, note that by the definition of the incremental variables $\tilde{x}, \tilde{\phi}, \tilde{\Phi}$ the error dynamics read

$$\begin{aligned} \tilde{x}^+ &= \bar{A}\tilde{x} + \bar{B}\tilde{\psi} + C\tilde{\Phi} = \begin{bmatrix} \bar{A} & \bar{B} & C \end{bmatrix} \zeta, \\ \bar{A} &= A + BR_\omega, \\ \bar{B} &= -BN_{u\omega}R. \end{aligned} \tag{24}$$

We introduce the following projection matrices

$$\begin{aligned}\Pi_\nu &= \begin{bmatrix} \mathrm{I}_{n_x} & 0 & 0 \\ 0 & \mathrm{I}_{n_\phi} & 0 \\ RN_{\nu x} & \mathrm{I}_{n_\phi} - R & 0, \end{bmatrix} \in \mathbb{R}^{n_\xi \times (n_x+n_\phi+n_q)}, \\ \Pi_s &= \begin{bmatrix} E & 0 & 0 \\ 0 & 0 & \mathrm{I}_{n_q} \end{bmatrix} \in \mathbb{R}^{(n_x+n_q)\times(n_x+n_\phi+n_q)},\end{aligned} \tag{25}$$

satisfying $\xi = \Pi_\nu \zeta$ and $\mathrm{col}(E\tilde{x}, \tilde{\Phi}) = \Pi_s \zeta$.

We are now ready to state the main result of the paper.

Theorem 1. *Consider system* (7) *under the controller* π_{ETM} *in* (14). *If there exist matrices* $P = P^\top \succ 0 \in \mathbb{R}^{n_x \times n_x}$, $\mathbf{R} \succ 0$, $Q \in \mathbb{R}^{n_x \times n_q}, W \in \mathbb{R}^{n_q \times n_q}$, $Z^i \in \mathbb{R}^{n_\phi \times n_x}$ X^i, N_1^i, N_2^i, N_3^i, *diagonal matrices* $T^i \succ 0$ *and vectors* $\alpha^i > 0 \in \mathbb{R}^{n_{\phi^i}}$ *for* $i = 1, \dots, l+1$, *such that the matrix inequalities* (26), (20) *and* (2) *hold for each* $i = 1, \dots, l+1$ *with* Ω^i *as in* (16), $\mathbf{X}$ *as in* (22), $\mathrm{v}_j^i = \min(|-\bar{\mathrm{v}}_j^i - \nu_{*,j}^i|, |\bar{\mathrm{v}}_j^i - \nu_{*,j}^i|)$, $\mu_i = \min(|-\underline{\mu}_i - y_i^*|, |\bar{\mu}_i - y_i^*|)$, *then* $(x_*, \mathbf{0})$ *is a LES equilibrium point with ROA including the ellipsoid* $\mathcal{E}(P, x_*) = \left\{x \in \mathbb{R}^{n_x}, \boldsymbol{\eta} \in \mathbb{R}^{l+1} : \tilde{x}^\top P \tilde{x} + \mathrm{He}\left\{\mathbf{1}_{l+1}^\top \boldsymbol{\eta}\right\} \le 1\right\}$.

Proof: We start by showing the implications of (26b), (26c) and (20). Inequality

$$\left[\alpha_j^i (\mathrm{v}_j^i)^{-2} - T_{j,j}^i\right] (\mathrm{v}_j^i)^2 \left[\alpha_j^i (\mathrm{v}_j^i)^{-2} - T_{j,j}^i\right] \ge 0$$

implies $(T_{j,j}^i)^2 (\mathrm{v}_j^i)^2 \ge 2\alpha_j^i T_{j,j}^i - {\alpha_j^i}^2 (\mathrm{v}_j^i)^{-2}$ for all α_j^i. Therefore, the satisfaction of (26b) yields

$$\begin{bmatrix} P & {Z_j^i}^\top \\ \star & (T_{j,j}^i)^2 (\mathrm{v}_j^i)^2 \end{bmatrix} \succeq \begin{bmatrix} P & {Z_j^i}^\top \\ \star & 2\alpha_j^i T_{j,j}^i - {\alpha_j^i}^2 (\mathrm{v}_j^i)^{-2} \end{bmatrix} \succeq 0.$$

Consequently, by the definition of Z^i qwe have

$$\begin{bmatrix} P & 0 & (T_{j,j}^i G_j^i)^\top \\ 0 & 2\,\mathrm{I}_{l+1} & 0 \\ \star & 0 & (T_{j,j}^i)^2 (\mathrm{v}_j^i)^2 \end{bmatrix} \succeq 0.$$

If $\boldsymbol{\eta}$ is non-negative, $\sqrt{\boldsymbol{\eta}}$ is real and by pre- and post-multiplying the above inequality by $\mathrm{col}(\tilde{x}, \sqrt{\boldsymbol{\eta}}, 1)$ and its transpose, a Schur's complement yields

$$\begin{bmatrix} \tilde{x} \\ \sqrt{\boldsymbol{\eta}} \end{bmatrix}^\top \begin{bmatrix} P & 0 \\ 0 & 2\,\mathrm{I}_{l+1} \end{bmatrix} \begin{bmatrix} \tilde{x} \\ \sqrt{\boldsymbol{\eta}} \end{bmatrix} \succeq \tilde{x}^\top \frac{(G_j^i)^\top (G_j^i)}{(\mathrm{v}_j^i)^2} \tilde{x}.$$

This ensures $\mathcal{E}(P, x_*) \subseteq \mathcal{S} \times \mathbb{R}^{l+1}$ with $\mathcal{S}$ defined as in Lemma 1. Similarly, (26c) implies

$$\begin{bmatrix} P & 0 & E_i^\top \\ 0 & 2\,\mathrm{I}_{l+1} & 0 \\ E_i & 0 & {\widehat{\mu}_i}^2 \end{bmatrix} \succeq 0.$$

Hence, by expressing $\tilde{y}_i = E_i \tilde{x}$ and pre- and post-multiplying the above inequality by $\mathrm{col}(\tilde{x}, \sqrt{\boldsymbol{\eta}}, 1)$ we have

$$\begin{bmatrix} \tilde{x} \\ \sqrt{\boldsymbol{\eta}} \end{bmatrix}^\top \begin{bmatrix} P & 0 \\ 0 & 2\,\mathrm{I}_{l+1} \end{bmatrix} \begin{bmatrix} \tilde{x} \\ \sqrt{\boldsymbol{\eta}} \end{bmatrix} \succeq \tilde{x}^\top \frac{{E_i}^\top E_i}{{\widehat{\mu}_i}^2} \tilde{x} = \frac{{y_i}^\top y_i}{{\widehat{\mu}_i}^2} \succeq 0.$$

Once again, this ensures $\mathcal{E}(P, x_*) \subseteq \bar{\mathcal{S}} \times \mathbb{R}^{l+1}$ with $\bar{\mathcal{S}}$ defined in Assumption 1. Thus (26b), (26c) imply $\mathcal{E}(P, x_*) \subseteq \left\{\mathcal{S} \cap \bar{\mathcal{S}}\right\} \times \mathbb{R}^{l+1}$. Finally, if (20) holds for each $i = 1, \dots, l+1$, Lemma 2 guarantees that $\boldsymbol{\eta} > 0$ for all $(x, \boldsymbol{\eta}) \in \mathcal{S}$, as discussed in Remark 1. Therefore, $\boldsymbol{\eta} \ge 0$ for all $(x, \boldsymbol{\eta}) \in \mathcal{E}(P, x_*)$.

We now move to the stability analysis. As shown above, $\mathcal{E}(P, x_*) \subseteq \left\{S \cap \bar{S}\right\} \times \mathbb{R}_{\ge 0}^{l+1}$. Therefore, for $(x, \boldsymbol{\eta}) \in \mathcal{E}(P, x_*)$, consider the following candidate Lyapunov function $V = \tilde{x}^\top P \tilde{x} + \mathrm{He}\left\{\mathbf{1}_{l+1}^\top \boldsymbol{\eta}\right\}$. Note that, by the definition of Π_s in (25), we have

$$\begin{bmatrix} \tilde{x} \\ \tilde{\psi} \\ \tilde{\Phi}(Ex) \end{bmatrix}^\top \Pi_s^\top \begin{bmatrix} S & Q \\ \star & W \end{bmatrix} \Pi_s \begin{bmatrix} \tilde{x} \\ \tilde{\psi} \\ \tilde{\Phi}(Ex) \end{bmatrix} \ge 0, \tag{27}$$

for all $y = Ex \in \bar{S}$. Moreover, by the definition of Π_ν in (25) and the Kronecker's product properties, the following equalities hold

$$\begin{aligned} &\zeta^\top (\mathbf{1}_{l+1} \otimes \Pi_\nu)^\top \mathrm{He}\{\mathbf{X}\} (\mathbf{1}_{l+1} \otimes \Pi_\nu) \zeta \\ &= (\mathbf{1}_{l+1} \otimes \Pi_\nu \zeta)^\top \mathrm{He}\{\mathbf{X}\} (\mathbf{1}_{l+1} \otimes \Pi_\nu \zeta) \\ &= (\mathbf{1}_{l+1} \otimes \xi)^\top \mathrm{He}\{\mathbf{X}\} (\mathbf{1}_{l+1} \otimes \xi) \\ &= \mathbf{1}_{l+1}^\top (\mathrm{I}_{l+1} \otimes \xi)^\top \mathrm{He}\{\mathbf{X}\} (\mathbf{1}_{l+1} \otimes \xi) = \mathbf{1}_{l+1}^\top \boldsymbol{\Psi}_{\mathbf{X}}. \end{aligned} \tag{28}$$

Therefore, if (26a) holds, its pre- and post- multiplication by ζ and its transpose with ζ as in (24), combined with (27) and (28) yields

$$\begin{aligned} &\begin{bmatrix} \tilde{x} \\ \tilde{\psi} \\ \tilde{\Phi} \end{bmatrix}^\top \left(\begin{bmatrix} \bar{A}^\top \\ \bar{B}^\top \\ C^\top \end{bmatrix} P \begin{bmatrix} \bar{A} & \bar{B} & C \end{bmatrix} - \begin{bmatrix} P & 0 & 0 \\ 0 & 0 & 0 \\ 0 & 0 & 0 \end{bmatrix} \right) \begin{bmatrix} \tilde{x} \\ \tilde{\psi} \\ \tilde{\Phi} \end{bmatrix} + \\ &\qquad + \mathrm{He}\left\{\mathbf{1}_{l+1}^\top \left[(\mathbf{R} - \mathrm{I}_{l+1})\boldsymbol{\eta} - \boldsymbol{\Psi}_{\mathbf{X}}\right]\right\} < 0. \end{aligned}$$

By expanding the products, we obtain

$$(\tilde{x}^+)^\top P \tilde{x}^+ - \tilde{x}^\top P \tilde{x} + \mathrm{He}\left\{\mathbf{1}_{l+1}^\top (\boldsymbol{\eta}^+ - \boldsymbol{\eta})\right\} = V^+ - V < 0.$$

Therefore, $\mathcal{E}(P, x_*)$ is forward invariant, and all trajectories starting inside such a set converge to $(x_*, \mathbf{0})$, thus concluding the proof. □

3.3 Optimizing the ETM parameters

The LMI conditions in Theorem 1 leave room for performance optimization of the proposed ETM scheme. For instance, different choices of $\mathbf{X}$ and $\mathbf{R}$ satisfying (20) and (26) provide different triggering frequencies due to (22). Moreover, the choice of $\mathbf{R}$ affects also the convergence rate of the extended closed-loop system, see (Girard, 2015). Hence, we now propose a corollary result aimed at improving performance of the triggered closed loop.

Corollary 1. *Consider system* (7) *under the controller* π_{ETM} *in* (14). *If there exist matrices* $P = P^\top \succ 0 \in \mathbb{R}^{n_x \times n_x}$, $\mathbf{R} \succ 0$, $Q \in \mathbb{R}^{n_x \times n_q}, W \in \mathbb{R}^{n_q \times n_q}$, $Z^i \in \mathbb{R}^{n_\phi \times n_x}$ X^i, N_1^i, N_2^i, N_3^i, *diagonal matrices* $T^i \succ 0$, *vectors* $\alpha^i > 0 \in \mathbb{R}^{n_{\phi^i}}$ *for* $i = 1, \dots, l+1$, *a diagonal matrix* $\Sigma \succ 0$, *positive scalars* β^i *for each* $i = 1, \dots, l+1$ *and* $\gamma \in [0, 1)$ *such that* (2) *holds and solution to*

$$\begin{aligned} \min\ & \mathrm{tr}\, P + \mathrm{tr}\, \Sigma + \sum_{i=1}^{l+1} \beta^i \\ s.t.\quad & (26), \\ & \mathbf{R} \preceq \gamma\, \mathrm{I}_{l+1} \\ & \Xi + \Sigma \succeq 0, \\ & (21), \quad i = 1, \dots, l+1, \\ & \begin{bmatrix} -\beta^i \mathrm{I}_{n_{\xi^i}} & X^i \\ {X^i}^\top & -\mathrm{I}_{n_{\xi^i}} \end{bmatrix} \preceq 0, \quad i = 1, \dots, l+1, \end{aligned} \tag{29}$$

S with Ω^i *as in* (16), $\mathbf{X}$ *as in* (22), $\mathrm{v}_j^i = \min(|-\bar{\mathrm{v}}_j^i - \nu_{*,j}^i|, |\bar{\mathrm{v}}_j^i - \nu_{*,j}^i|)$, $\mu_i = \min(|-\underline{\mu}_i - y_i^*|, |\bar{\mu}_i - y_i^*|)$, *then*

$$\Xi = \left[\begin{array}{c|c} \begin{bmatrix}\bar{A}^\top \\ \bar{B}^\top \\ C^\top\end{bmatrix} P \begin{bmatrix}\bar{A} & \bar{B} & C\end{bmatrix} - \begin{bmatrix}P & 0 & 0 \\ 0 & 0 & 0 \\ 0 & 0 & 0\end{bmatrix} - (\mathbf{1}_{l+1} \otimes \Pi_\nu)^\top \mathrm{He}\{\mathbf{X}\} (\mathbf{1}_{l+1} \otimes \Pi_\nu) + \Pi_s^\top \begin{bmatrix}S & Q \\ \star & W\end{bmatrix} \Pi_s & 0 \\ \hline 0 & 2(\mathbf{R} - \mathrm{I}_{l+1}) \end{array}\right] \prec 0, \quad (26a)$$

$$\begin{bmatrix} P & {Z_j^i}^\top \\ \star & 2\alpha_j^i T_{j,j}^i - {\alpha_j^i}^2 (\mathrm{v}_j^i)^{-2} \end{bmatrix} \succeq 0, \qquad \forall i \in \{1, \dots, l+1\}, j \in \left\{1, \dots, n_{\phi^i}\right\}, \quad (26b)$$

$$\begin{bmatrix} P & {E_i}^\top \\ \star & {\mu_i}^2 \end{bmatrix} \succeq 0, \qquad \forall i \in \{1, \dots, n_q\}. \quad (26c)$$

Setup	λ_{l^1}	λ_{l^2}	λ_{l^3}	λ_u	$\mathcal{L}_{\text{tot}}$	$\mathbb{V}(\mathcal{E}(P, x_*))$
$\mathcal{C}_\Omega^s$	94.57	54.29	45.43	29.14	64.39	80.28
$\mathcal{C}_\Omega^d$	86.57	**32.86**	32.57	27.71	50.43	65.78
$\mathcal{C}_X^s$	45.43	33.43	33.43	34.57	37.40	**81.33**
$\mathcal{C}_X^d$	43.43	**32.86**	**32.29**	**25.43**	36.08	**81.33**
$\mathcal{C}_{\lvert X\rvert}^s$	35.71	35.71	35.71	36.57	35.72	80.89
$\mathcal{C}_{\lvert X\rvert}^d$	**34.29**	33.71	32.86	26.29	**33.54**	80.89

Table 1. Comparison of update rates and volume of ROA approximation. Results are drawn out by the mean of 100 simulations with the same initial conditions among configurations

.

$(x_*, \mathbf{0})$ *is a LES equilibrium point and* $\mathcal{E}(P, x_*)$ *is an inner approximation of its ROA.*

The additional constraints in Corollary 1 serve the following purposes:

- Minimization of the trace of P maximizes the volume of the ellipsoid $\mathcal{E}(P, x_*)$, thereby increasing the ROA (Durieu et al., 1996).
- Minimization of the trace of Σ pushes (26a) towards infeasibility, thus reducing the decay rate of the Lyapunov function. This choice encourages event sparsification, as frequent updates are not needed to steer trajectories to the equilibrium sufficiently fast.
- The introduction of γ is used as an upper bound to avoid the undesired side-effect of the ETM dynamics setting the overall system decay rate. In other words, the combination of γ and Σ ensures the ETM dynamics are sufficiently fast not to dominate the system decay rate, yet sufficiently slow to reduce the generation of events in view of (22).
- Applying the Schur complement to the top-left block of the last condition in (29), we obtain

$$ {X^i}^\top X^i \preceq \beta^i \, \mathrm{I}_{n_{\xi^i}}, \qquad i = 1, \dots, l+1 $$

  Therefore, minimization of β^i minimizes the norm of X^i, thus reducing the number of events given (22).

It is important to discuss the vectors α^i in (26b). The elements of each α^i appear as bilinear terms in (26), and therefore, they must be fixed to ensure convex conditions. However, selecting these vectors presents a challenge, as they significantly influence the conservatism of the solution and are computationally expensive to determine through parametric search, given the high number of parameters involved. In our implementation, we fix $\alpha^i = \alpha \, \mathbf{1}_{n_{\phi^i}}$ for all $i = \{1, \dots, l+1\}$, with α a positive scalar. This simplifies the problem at the cost of increased conservatism. This approach reduces the problem to a generalized eigenvalue problem, which can be efficiently solved using search algorithms such as bisection or the *golden ratio search*. The latter offers minor improvements over bisection while enhancing computational efficiency.

4. SIMULATIONS

We consider the problem of stabilization of a sampled, input-saturated inverted pendulum system with mass $m = 0.15kg$, length $l = 0.5m$, damping coefficient $\mu = 0.05Nms/rad$, gravitational acceleration $g = 9.81m/s^2$. To robustly compensate for the constant disturbance d, an integrator is added to the system's dynamics (Zoboli et al., 2023). A locally stabilizing NN controller can be obtained using techniques such as (Yin et al., 2021). The discrete-time (DT) model of the system is given in the form of (7) as

$$x = \begin{bmatrix}\theta \\ \dot{\theta} \\ z\end{bmatrix} \quad A = \begin{bmatrix}1 & dt & 0 \\ \frac{g}{l}dt & 1 - \frac{\mu}{ml^2}dt & 0 \\ 1 & 0 & 1\end{bmatrix} \quad B = \begin{bmatrix}0 \\ \frac{\bar{\tau}}{ml^2}dt \\ 0\end{bmatrix}$$
$$C = \begin{bmatrix}0 \\ \frac{g}{l}dt \\ 0\end{bmatrix} \quad D = \begin{bmatrix}0 \\ 0 \\ -1\end{bmatrix} \quad E = [1 \ 0 \ 0] \quad (30)$$

Note that such a choice for A, D imposes d to be a reference for θ, namely, $\theta_* = d$. The maximum input torque is $\bar{\tau} = 5Nm$, the sampling time is $dt = 0.02s$ and the nonlinearity is $\Phi(Ex) = \sin(Ex) - Ex$. This nonlinearity satisfies the quadratic abstractions

$$\begin{bmatrix}y \\ sin(y) - y\end{bmatrix}^\top \begin{bmatrix}0 & -1 \\ -1 & -2\end{bmatrix} \begin{bmatrix}y \\ sin(y) - y\end{bmatrix} > 0, \quad \forall y \in [-\pi, \pi],$$

see, e.g. (Junnarkar et al., 2024b). This matches (3) with $y = Ex$ and $y_* = 0$. Therefore, by selecting the origin as the reference for θ as defined by (30), the previous conditions hold globally due to the periodicity of the *sin* function. By selecting $n_q = 1, S = 0, Q = -1, W = -2$, we avoid adding condition (26c) in the LMI problem formulation. Given the inclusion of the maximum torque $\bar{\tau}$ in B, the saturation level $\mathtt{u}$ is set to 1. Similarly, all

activation functions' saturation level are also set to 1. This is consistent with common deep reinforcement learning frameworks. The controller π is structured as an MLP with $l = 3$ layers of sizes $n_{\phi_1} = n_{\phi_2} = n_{\phi_3} = 32$. By imposing all $\alpha^i = 0.053 \cdot \mathbf{1}$ and $\gamma = 0.86$ we compare 6 significant ETM configurations:

- $\mathcal{C}^s_\Omega$: Triggering conditions of (19) adapted to include saturation with static ETM minimizing $\operatorname{tr} P$;
- $\mathcal{C}^d_\Omega$: Triggering conditions of (19) adapted to include saturation with dynamic ETM minimizing $\operatorname{tr} P + \operatorname{tr} \Sigma$;
- $\mathcal{C}^s_X$: Our proposed triggering conditions with static ETM minimizing $\operatorname{tr} P + \operatorname{tr} \Sigma$;
- $\mathcal{C}^d_X$: Our proposed triggering conditions with dynamic ETM minimizing $\operatorname{tr} P + \operatorname{tr} \Sigma$;
- $\mathcal{C}^s_{|X|}$: Our proposed triggering conditions with static ETM minimizing $\operatorname{tr} P + \operatorname{tr} \Sigma + \sum_{i=1}^{l+1} \beta^i$;
- $\mathcal{C}^d_{|X|}$: Our proposed triggering conditions with dynamic ETM minimizing $\operatorname{tr} P + \operatorname{tr} \Sigma + \sum_{i=1}^{l+1} \beta^i$.

The results of such comparison are highlighted in Table 1. The data is obtained by averaging 100 simulations starting from different initial conditions (identical among configurations) such that $(x_0, \boldsymbol{\eta}_0) \in \mathcal{E}(P_{\mathcal{C}^d_\Omega}, x_*)$, i.e., valid also for the more conservative result. The simulations are run for $n_{\text{steps}} = 350$ to ensure that all configurations reach the arbitrarily small Lyapunov function threshold of 10^{-15}, which occurs within approximately 300 steps for each case. This uniform stopping criterion accommodates all configurations, which exhibit comparable decay rates The update rates of the layers are denoted by λ_{l^i}, where $\lambda_u = \lambda_{l^4}$, representing the percentage of total steps the i^{th} layer has been updated. $\mathcal{L}_{\text{tot}}$ indicates the overall percentage of triggered activation functions across the entire controller throughout the simulation. This metric directly reflects the computational savings achieved by the ETM. These values are calculated as follows:

$$\lambda_{l^i} = \frac{n_{\text{events}^i}}{n_{\text{steps}}} \cdot 100, \qquad \mathcal{L}_{\text{tot}} = \frac{\sum_{i=1}^{l+1} \lambda_{l^i} \cdot n_{\phi^i}}{n_\phi},$$

where n_{events^i} represents the number of events generated for layer i . The volume of the ellipsoid $\mathcal{E}(P, x_*)$ is a direct indication of the conservatism of the solution and is computed as

$$\mathbb{V}(\mathcal{E}(P, x_*)) = \frac{4}{3} \frac{\pi}{\sqrt{\det P}}.$$

Compared to $\mathcal{C}^s_\Omega$ (approximately corresponding to the solution in (Tarbouriech et al., 2024)), Table 1 highlights that the controller's update rate decreases significantly with each proposed improvements. Similarly, the proposed methods show a more uniform event pattern across layers. Refining triggering conditions using Lemma 2, especially in the dynamic case, further reduces the update rate while addressing the conservatism of $\mathcal{C}^d_\Omega$. Comparing $\mathcal{C}^s_X, \mathcal{C}^d_X$ with $\mathcal{C}^s_{|X|}, \mathcal{C}^d_{|X|}$ highlights a trade-off between computational efficiency and the ROA approximation size. The final update rates are reduced by up to 70% compared to a standard periodic controller, significantly lowering the computational load and enabling implementation on resource-constrained systems.

Figures 3,-6 depict in more detail a trajectory under $\mathcal{C}^d_{|X|}$ with

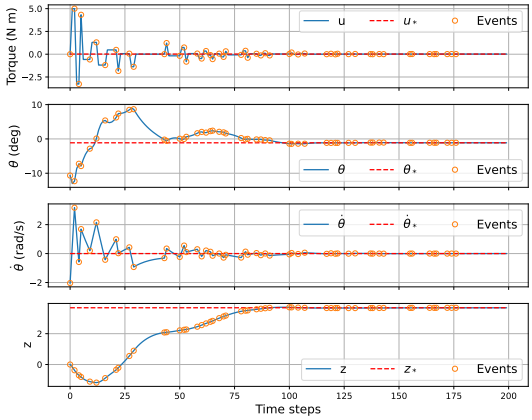

Fig. 3. First 200 steps evolution of u, x

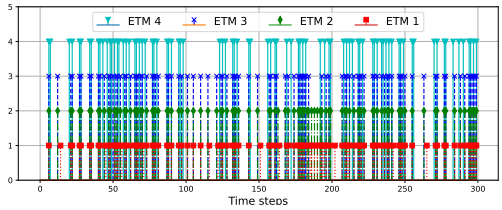

Fig. 4. Events occurring in first 300 steps

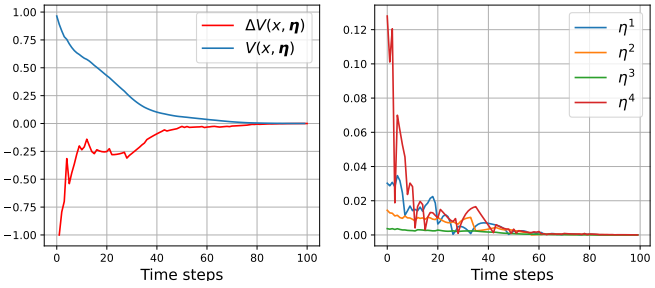

Fig. 5. First 100 steps evolution of V and normalized ΔV, along with η dynamic thresholds

$$x_0 = \begin{bmatrix} -10.67^\circ \\ -2.04\ rad/s \\ 0.0 \end{bmatrix}; \quad \boldsymbol{\eta}_0 = 0.001 \cdot \mathbf{1}; \quad d = -1.13^\circ.$$

Even if a non-zero reference d does not ensure the local quadratic abstraction (3) holds globally, the guaranteed exponential stability under the triggering scheme ensures robustness (and therefore convergence) of the closed loop thanks to the integrator dynamics (Zoboli et al., 2023).

5. CONCLUSIONS AND FUTURE WORKS

In this work, we presented a dynamic ETM scheme to reduce the computational burden of neural network layers evaluations. We focused on input-saturated partially linear systems controlled by stabilizing Multi-Layer Perceptron networks with saturation activation functions. By using Finsler's lemma and dynamic triggering thresholds, we proposed multiple improvements of existing methods exploiting linear matrix inequalities. We experimentally validated our approaches, that showed reduced conservatism

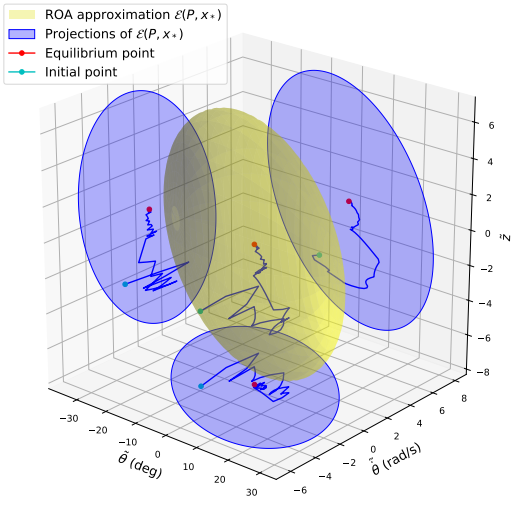

Fig. 6. Trajectory of the system within $\mathcal{E}(P, x_*)$ and with respect to its projections

with respect to existing solutions. Future work will focus on refining the proposed conditions, in the attempt of obtaining a completely convex methodology. Additionally, we aim to explore the inclusion of nonlinear ETM dynamics, inspired by (Alessandri and Zaccarian, 2018).

REFERENCES

Alessandri, A. and Zaccarian, L. (2018). Stubborn state observers for linear time-invariant systems. *Automatica*, 88, 1–9.

Boyd, S., El Ghaoui, L., Feron, E., and Balakrishnan, V. (1994). *Linear matrix inequalities in system and control theory*. SIAM.

Chow, Y., Nachum, O., Duenez-Guzman, E., and Ghavamzadeh, M. (2018). A Lyapunov-based approach to safe reinforcement learning. *Advances in Neural Information Processing Systems (NEURIPS)*, 31.

de Souza, C., Girard, A., and Tarbouriech, S. (2023a). Event-triggered neural network control using quadratic constraints for perturbed systems. *Automatica*, 157, 111237.

de Souza, C., Tarbouriech, S., and Girard, A. (2023b). Event-triggered neural network control for LTI systems. *IEEE Control Systems Letters*, 7, 1381–1386.

Dimarogonas, D.V. and Johansson, K.H. (2009). Event-triggered control for multi-agent systems. In *IEEE Conference on Decision and Control (CDC)*, 7131–7136.

Durieu, C., Polyak, B.T., and Walter, E. (1996). Trace versus determinant in ellipsoidal outer-bounding, with application to state estimation. *IFAC Proceedings Volumes*, 29(1), 3975–3980.

Girard, A. (2015). Dynamic triggering mechanisms for event-triggered control. *IEEE Transactions on Automatic Control*, 60(7), 1992–1997.

Hu, S., Yue, D., Xie, X., Ma, Y., and Yin, X. (2016). Stabilization of neural-network-based control systems via event-triggered control with nonperiodic sampled data. *IEEE Transactions on Neural Networks and Learning Systems*, 29(3), 573–585.

Junnarkar, N., Arcak, M., and Seiler, P. (2024a). Stability margins of neural network controllers. *arXiv preprint arXiv:2409.09184*.

Junnarkar, N., Arcak, M., and Seiler, P. (2024b). Synthesizing neural network controllers with closed-loop dissipativity guarantees. *arXiv preprint arXiv:2404.07373*.

Meijer, T., Scheres, K., van den Eijnden, S., Holicki, T., Scherer, C., and Heemels, M. (2024). A unified non-strict Finsler lemma. *IEEE Control Systems Letters*.

Mu, C., Wang, K., and Qiu, T. (2022). Dynamic event-triggering neural learning control for partially unknown nonlinear systems. *IEEE Transactions on Cybernetics*, 52(4), 2200–2213.

Postoyan, R., Tabuada, P., Nešić, D., and Anta, A. (2015). A framework for the event-triggered stabilization of nonlinear systems. *IEEE Transactions on Automatic Control*, 60(4), 982–996.

Sun, D., Jha, S., and Fan, C. (2021). Learning certified control using contraction metric. In *Conference on Robot Learning*, 1519–1539. PMLR.

Tabuada, P. (2007). Event-triggered real-time scheduling of stabilizing control tasks. *IEEE Transactions on Automatic control*, 52(9), 1680–1685.

Tarbouriech, S., de Souza, C., and Girard, A. (2024). Layers update of neural network control via event-triggering mechanism. In *Hybrid and Networked Dynamical Systems: Modeling, Analysis and Control*, 253–272. Springer.

Tarbouriech, S., Garcia, G., Gomes da Silva Jr, J.M., and Queinnec, I. (2011). *Stability and stabilization of linear systems with saturating actuators*. Springer Science & Business Media.

Wang, R. and Manchester, I.R. (2022). Youla-REN: Learning nonlinear feedback policies with robust stability guarantees. In *American Control Conference (ACC)*, 2116–2123. IEEE.

Yang, L., Dai, H., Shi, Z., Hsieh, C.J., Tedrake, R., and Zhang, H. (2024). Lyapunov-stable neural control for state and output feedback: A novel formulation for efficient synthesis and verification. *arXiv preprint arXiv:2404.07956*.

Yin, H., Seiler, P., and Arcak, M. (2021). Stability analysis using quadratic constraints for systems with neural network controllers. *IEEE Transactions on Automatic Control*, 67(4), 1980–1987.

Zoboli, S., Andrieu, V., Astolfi, D., Casadei, G., Dibangoye, J.S., and Nadri, M. (2021). Reinforcement learning policies with local LQR guarantees for nonlinear discrete-time systems. In *IEEE Conference on Decision and Control (CDC)*, 2258–2263. IEEE.

Zoboli, S., Astolfi, D., and Andrieu, V. (2023). Total stability of equilibria motivates integral action in discrete-time nonlinear systems. *Automatica*, 155, 111154.